Time-Frequency distributions with generalized complex lag argument

Cedric Cornu, Srdjan Stankovic, Cornel Ioana, André Quinquis, Ljubisa Stankovic

Generalized Representation of Phase Derivatives for Regular Signals

Cédric Cornu, *PhD Student*, Srdjan Stanković, *Member, IEEE,* Cornel Ioana, *Member, IEEE,*
André Quinquis, *Senior Member, IEEE,* and Ljubisa Stanković, *Senior Member, IEEE*

Abstract— **This paper introduces a new generalized complex lag moment which produces "time-phase derivatives" distributions. For the choice of the "time-first phase derivative" which stands for time-frequency representation, this distribution can be seen as a form of the Wigner-Ville distribution. Moreover, this generalization leads to distributions with highly reduced inner interferences caused by the nonlinearity of the signal's phase. It can also be seen as a polynomial distribution since the distribution of Nth order produces no inner interferences for polynomial phase law of order N. Implementation problems of this distribution are presented. The results are illustrated by examples.**

Index Terms— **Time-frequency, phase non linearity, representation, analytic continuation.**

I. INTRODUCTION

A General form of complex lag distributions, that estimates any order of instantaneous phase derivative, is introduced. This class of distributions is based on the complex lag argument. It will be referred to as a general form of the complex time distributions. Beside the fact that these distributions provide estimation of any arbitrary order of instantaneous phase derivative, a high concentration of the distribution along the chosen phase derivative can be achieved. Note that the first phase derivative is the instantaneous frequency. Thus, special cases of this class of distributions are time frequency distributions. They have been intensively investigated during last fifteen years, [1], [2], since they play an important role in the instantaneous frequency estimation. Distributions, introduced by using the approach given here, are highly concentrated in the time-frequency plane and they provide accurate instantaneous frequency estimation, even in the case of significant instantaneous frequency variation within only a few signal samples. Note that the physical meaning of the first derivative of signal phase function is the instantaneous frequency itself. Recently, in the paper [3], O'Shea analyzes the second order phase derivative, i.e. the instantaneous frequency rate. The estimation introduced in [3] can be obtained with a slight modification of a particular form of the generalized complex lag distribution. In addition, better instantaneous frequency rate concentration can be achieved by using higher order time frequency rate distributions belonging to the proposed class of distributions. Distributions providing the third instantaneous phase derivative are also introduced and analyzed.

The paper is organized through five sections. The concept and theory of the proposed class of distributions are presented in Section II. The theory is illustrated by various examples in Section III. The problem of numerical implementation is considered in Section IV. The most interesting specific distributions, belonging to the proposed class of distributions, are introduced and tested in Section V. Special attention is devoted to the cases of the first, the second and the third phase derivative. In the case of first phase derivative (frequency), superiority of the proposed approach is proven by introducing the sixth order distribution [4], that estimates the instantaneous frequency, even when it could not be achieved by using other time frequency tools.

II. INSTANTANEOUS PHASE DERIVATIVES

A. Concept

The ideal representation of an arbitrary instantaneous phase derivative can be written in the form:

$$IPD_K(t,\Omega) = \delta(\Omega - \Phi^{(K)}(t))$$

where Ω is the axis which corresponds to the Kth derivative of phase function $\Phi(t)$. The distribution which provides this representation will be called, in general, the time-phase derivatives distribution. Note that, for $K = 1$, the instantaneous frequency representation is obtained as:

$$IPD_1(t,\omega) = \delta(\omega - \Phi'(t)) \tag{1}$$

where $\Omega \equiv \omega$ and $\Phi'(t)$ is the first phase derivative, i.e. instantaneous frequency. This representation can be achieved by using well known time-frequency distributions.

For $K = 2$ instantaneous frequency rate follows:

$$IPD_2(t,\Omega) = \delta(\Omega - \Phi^{(2)}(t)) \tag{2}$$

where Ω is the frequency rate axis. Instantaneous frequency rate representation can be provided by using, recently defined, time-frequency rate distributions.

Note that these two special cases have already been studied, intensively for the first one, while the case $K = 3$ has not been considered yet. A reason for this could be the elaborate forms of distributions even for the first two cases. Namely, ideal representations given by equations (1) and (2) can not generally be achieved by using any time-frequency or time-frequency rate distribution. Terms which cause spreading of the distribution concentration, around the instantaneous phase derivative, are inner interference terms. For $K = 1$, they depend on $\left\{\Phi^{(i)}(t)\right\}_i$, for $i \geq 2$. Note that for the spectrogram: $i = 2, 3, ...$, while for the Wigner distribution: $i = 3, 5, 7, ...$

Distribution proposed in the next section provides not only an arbitrary instantaneous phase derivative representation, but also a very high distribution concentration.

Observe that the energetic distributions should provide representation in the form:

$$IPD_K(t, \Omega_k) = A^2 \delta(\Omega_K - \Phi^{(K)}(t))$$

where A is the amplitude of the signal $s(t) = Ae^{j\Phi(t)}$. Thus, the signal energy is concentrated along the Kth phase derivative. Most of the commonly used time-frequency and time-frequency rate distributions satisfy this property.

The distribution which provides instantaneous K^{th} phase derivative is introduced in the next subsection.

B. Introducing generalized complex lag time-phase derivatives distribution

In the sequel we will show that, by using the complex-lag argument concept, a set of powerful distributions in signal analysis can be defined. In order to reduce inner interferences in time-frequency representation of highly nonstationary signals, the complex lag argument was introduced in [5] . Distributions with generalized complex lag moment (GCM), that provide any instantaneous phase derivatives estimation, are defined in this section, (8). The distributions as: the short time Fourier transform, the Wigner-Ville distribution (WVD), or O'Shea's time-frequency rate estimator, are obtained as special cases. However, it is important to emphasize that this concept provides the new, highly concentrated, distributions along the arbitrary phase derivative.

Let us consider a signal in the form (3).

$$s(t) = Ae^{j\Phi(t)} \tag{3}$$

Assuming an analytic signal, (4), and using the Taylor's series expansion of the phase, we can write:

$$s(t + \tau) = Ae^{j\sum_k \Phi^{(k)}(t)\frac{\tau^k}{k!}} \tag{4}$$

Phase integration in the complex plane allows the focusing on a particular phase derivative, (5).

$$\Phi^{(k)}(t) = \frac{k!}{2\pi\tau^k} \int_0^{2\pi} \Phi(t + \tau e^{j\theta}) e^{-jk\theta} d\theta \tag{5}$$

Consider now the discrete form, which is used in numerical implementations. Taking $\{\omega_{N,k}\}$ as the Nth roots of unity, $\omega_{N,k} = e^{j2\pi k/N}$, we can note their interesting property:

$$\sum_{k=0}^{N-1} \omega_{N,k}^p = \begin{cases} N & \text{if } p = 0 \pmod N \\ 0 & \text{if not} \end{cases}$$

Using this property, it is possible to get rid of some terms in the expansion of $\Phi(t + \tau)$. After relatively simple derivation, we obtain:

$$\sum_{k=0}^{N-1} \Phi(t + \omega_{N,k}\tau)\omega_{N,k}^{N-K} = N \sum_{k=0}^{+\infty} \Phi^{(Nk+K)}(t) \frac{\tau^{Nk+K}}{(Nk+K)!} \tag{6}$$

$$\sum_{k=0}^{N-1} \Phi(t + \omega_{N,k}\tau)\omega_{N,k}^{N-K} = \Phi^{(K)}(t) \frac{N\tau^K}{K!} + Q(t, \tau) \tag{7}$$

Having in mind the unity roots, we can see that the expression (7) contains only the derivatives of order $Nk + K$. Thus, the first one is the Kth derivative of $\Phi(t)$. This is helpful in defining a new generalized complex lag moment:

$$GCM_N^K[s](t, \tau) = \prod_{k=0}^{N-1} s^{\omega_{N,k}^{N-K}} \left(t + \omega_{N,k} \sqrt[K]{\frac{K!}{N}\tau} \right) \tag{8}$$

where lag axis τ is generalized and normalized. The Fourier transform of the generalized complex lag moment produces the generalized complex lag distribution, associated to this moment:

$$GCD_N^K[s](t, \omega) = \mathfrak{F}_\tau \left[GCM_N^K[s](t, \tau) \right] \tag{9}$$

$$= \delta(\omega - \Phi^{(K)}(t)) \underset{\omega}{*} S(t, \omega) \tag{10}$$

Note that this distribution is concentrated along the Kth derivative of the phase. The spreading factor $S(t, \omega)$ has the form, (11):

$$S(t, \omega) = A\mathfrak{F}_\tau \left[e^{jQ(t,\tau)} \right] \tag{11}$$

The terms, related to the factor $Q(t, \tau)$, are results of the higher order phase derivatives. This factor has the form:

$$Q(t, \tau) = N \sum_{k=1}^{+\infty} \Phi^{(Nk+K)}(t) \frac{\tau^{\frac{Nk}{K}+1}}{(Nk+K)!} \left(\frac{K!}{N} \right)^{\frac{Nk}{K}+1} \tag{12}$$

In the ideal case, it should be zero. Observe that the first term appearing in the spreading factor is the phase derivative of order $K + N$, the second one is of order $K + 2N$, etc. Thus, the parameter N highly affects the factor $Q(t, \tau)$. It can be concluded that a high value of N reduces interferences, since $Q(t, \tau)$ is reduced and distribution concentration will be less sensitive to the higher order phase derivatives. In order to give a more comprehensive overview of this theoretical framework, several specific distributions which can be useful and illustrative examples are given in the next section.

III. SOME SPECIFIC DISTRIBUTIONS BELONGING TO THE GENERALIZED COMPLEX LAG DISTRIBUTION

A. Case $K = 1$: Instantaneous frequency representation-Time frequency distributions

Taking $K = 1$, we focus on the instantaneous frequency. In this case, the moment, (8), will have the form :

$$GCM_N^1[s](t, \tau) = \prod_{k=0}^{N-1} s^{\omega_{N,k}^*} \left(t + \frac{\omega_{N,k}}{N}\tau \right) \tag{13}$$

Depending on the parameter N, various forms of time-frequency distributions can be obtained. Let us begin with the first one, i.e. $N = 1$:

$$GCM_1^1[s](t, \tau) = s(t + \tau)$$

$$Q(t, \tau) = \Phi^{(2)}(t)\frac{\tau^2}{2!} + \Phi^{(3)}(t)\frac{\tau^3}{3!} + \dots$$

Here, the associated distribution is the short time Fourier transform (if a lag window is assumed). In the spreading factor $Q(t,\tau)$, all phase derivatives of order 2 and higher are implied. Thus, the short-time Fourier transform is well suited only for sinusoids localization.

For $N = 2$ we have:

$$GCM_2^1[s](t,\tau) = s(t+\frac{\tau}{2})s^{-1}(t-\frac{\tau}{2})$$
$$Q(t,\tau) = \Phi^{(3)}(t)\frac{\tau^3}{3!\,2^2} + \Phi^{(5)}(t)\frac{\tau^5}{5!\,2^4} + \cdots$$

This leads to a Wigner-Ville like distribution, with a difference in the second exponent of the moment which is -1 instead of a conjugate. However, both have the same effect on the phase. The first term appearing in $Q(t,\tau)$ is related to the third derivative. Indeed, the Wigner-Ville distribution can be used for ideal time frequency representation of linear chirp signals.

Suppose now $N = 4$:

$$GCM_4^1[s](t,\tau) = s(t+\frac{\tau}{4})s^{-1}(t-\frac{\tau}{4})s^{j}(t-j\frac{\tau}{4})s^{-j}(t+j\frac{\tau}{4})$$
$$Q(t,\tau) = \Phi^{(5)}(t)\frac{\tau^5}{5!\,4^4} + \Phi^{(9)}(t)\frac{\tau^9}{9!\,4^8} + \cdots$$

A distribution with the complex lag moment is obtained. We observe that the same complex lag moment, as the one in [5], is introduced. The complex time distribution (CTD) is ideally concentrated for polynomial instantaneous frequency laws of order 3 or less. However, it has been shown that it is still highly efficient for polynomial phase of order greater than 4, since the derivative coefficients in the spreading factor decay rapidly. For even N, the value -1 is always a root of the unity and the exponent with value -1 can be replaced with a conjugate, since the effect on the phase function will be the same. Hereafter, we will denote by $\widetilde{GCM_N^K}$ the moment GCM_N^K modified by replacing exponents -1 with conjugates. Thus, according to this notation the complex time distribution defined in [5] is $\widetilde{GCD_4^1}$. We can see that: $\int \widetilde{GCD_N^1}[s]d\omega = 1$ and $\int \widetilde{GCD_N^1}[s]d\tau = |s(t)|^2$.

Of course, it is possible to choose a higher value for N. For $N = 6$, highly concentrated, the sixth order time frequency distribution is obtained:

$$\{\omega_{6,k}\}_{k=0..5} = \left\{1; e^{j\frac{\pi}{3}}; e^{j\frac{2\pi}{3}}; -1; e^{j\frac{-2\pi}{3}}; e^{j\frac{-\pi}{3}}\right\}$$

$$GCM_6^1[s](t,\tau) = \prod_{k=0}^{5} s^{\omega_{6,k}^*}\left(t+\frac{\omega_{6,k}}{6}\tau\right)$$
$$Q(t,\tau) = \Phi^{(7)}(t)\frac{\tau^7}{7!\,6^5} + \Phi^{(13)}(t)\frac{\tau^{13}}{13!\,6^{12}} + \cdots$$

The first derivative appearing in the factor $Q(t,\tau)$ is of order 7. It means that a polynomial phase of order 6 or less will not produce any interferences in this distribution. For other signals, the interferences will be highly reduced, as a consequence of the very fast decreasing coefficients. Moreover, the position of

the sixth unity roots in the complex plane is an asset compared with those of fourth order distribution, for example. Indeed, we will stay closer to the real axis when computing the analytical continuation. As a consequence, the estimation error will be reduced and the computation will be less sensitive to noise.

In practical implementations, windowed forms of the time-frequency distributions are used. For the short time Fourier transform (or the spectrogram), the window size has to provide a trade off between time and frequency resolutions. For the pseudo Wigner-Ville distribution, the choice is made assuming the signal is like a linear chirp in the windows. Since this hypothesis is weaker than stationarity, the length of the window can be increased in comparison to the spectrogram. It is possible to further reduce a negative influence of the window size. Namely, window size can be increased, by using the generalized complex moment, proportionally to the parameter N. In this way, the accuracy could be, theoretically, highly improved. However, numerical implementations introduce some limits for window size in the complex lag moments based distributions. In the section with illustrative examples, we will rather use equal window's size to show interferences reduction.

B. Case $K = 2$: Time-frequency rate representation

The general form of the time-frequency rate distributions, with complex lag argument is given by:

$$GCM_N^2[s](t,\tau) = \prod_{k=0}^{N-1} s^{\omega_{N,k}^{N-2}}\left(t + \omega_{N,k}\sqrt[2]{\frac{2}{N}\tau}\right) \quad (14)$$

For $N = 2$ in (14), follows:

$$GCM_2^2[s](t,\tau) = s\left(t+\sqrt{\tau}\right)s\left(t-\sqrt{\tau}\right) \quad (15)$$

The relation (15) should be compared to the IFR representation, (16), and estimator, (17), introduced by Peter O'Shea.

$$CPD(t,\Omega) = \int_0^{+\infty} s(t+\tau)s(t-\tau)e^{j\Omega\tau^2}d\tau \quad (16)$$
$$IFR(t) = \underset{\Omega}{argmax}\left[CPD(t,\Omega)\right] \quad (17)$$

The representation (16) does not have a perfect concentration along IFR since it is never zero outside of the IFR path for any signal. This problem can be fixed using the substitution $\tau \to \sqrt{\tau}$, and the Fourier transform instead of the polynomial Fourier transform. With these modifications, the distribution GCD_2^2 is obtained.

Taking $N = 4$, we will introduce the new, fourth order, time-frequency rate distribution:

$$GCM_4^2[s](t,\tau) = s\left(t+\sqrt{\frac{\tau}{2}}\right)s\left(t-\sqrt{\frac{\tau}{2}}\right) \times$$
$$s^{-1}\left(t+j\sqrt{\frac{\tau}{2}}\right)s^{-1}\left(t-j\sqrt{\frac{\tau}{2}}\right) \quad (18)$$

$$\widetilde{GCM_4^2}[s](t,\tau) = s\left(t + \sqrt{\frac{\tau}{2}}\right) s\left(t - \sqrt{\frac{\tau}{2}}\right) \times$$
$$s^*\left(t + j\sqrt{\frac{\tau}{2}}\right) s^*\left(t - j\sqrt{\frac{\tau}{2}}\right) \quad (19)$$

The sixth order time-frequency rate distribution will be obtained by taking $N = 6$:

$$GCM_6^2[s](t,\tau) = \prod_{k=0}^{5} s^{\omega_{6,k}^4}\left(t + \omega_{6,k}\sqrt[2]{\frac{\tau}{3}}\right) \quad (20)$$

C. Case $K = 3$: Instantaneous third phase derivative representation

Note that, if we want to obtain distributions concentrated around thirth phase derivative, the parameter N must be $N \geq K$. Taking $N = 3$, we have:

$$\{\omega_{3,i}\} = \left\{1, e^{j2\pi/3}, e^{-j2\pi/3}\right\}$$

$$GCM_3^3[s](t,\tau) = \prod_{k=0}^{2} s\left(t + \omega_{3,k}\sqrt[3]{2\tau}\right) \quad (21)$$

It is easy to conclude that for $N = 4$ a better distribution concentration can be achieved. In this case we obtain the fourth order distribution:

$$GCM_4^3[s](t,\tau) = \prod_{k=0}^{3} s^{\omega_{4,k}}\left(t + \omega_{4,k}\sqrt[3]{\frac{3\tau}{2}}\right) \quad (22)$$

Taking $N = 6$, the sixth order distribution is introduced:

$$GCM_6^3[s](t,\tau) = \prod_{k=0}^{5} s^{(-1)^k}\left(t + \omega_{6,k}\sqrt[3]{\tau}\right) \quad (23)$$

IV. GCD IMPLEMENTATION

A. Analytical continuation

Computation of the signal's value in the complex plane must be done, based on the real signal samples. In mathematics, this concept is known as analytical continuation, [6]. A function $s(t)$ is said to be analytical if it can be written as a power series with a convergence disk of radius $R \neq 0$.

$$s(t) = \sum_{k=0}^{+\infty} a_k t^k \quad (24)$$

Moreover, the series equals its Taylor counterpart and, within its convergence radius, the function can be calculated for complex values.

$$s(t + \tau) = \sum_{k=0}^{+\infty} \frac{s^{(k)}(t)}{k!}\tau^k \quad (25)$$

For an analytic signal, the continuation can be written using the inverse Fourier transform.

$$s(t + jm) = \int_{+\infty}^{+\infty} S(f)e^{-2\pi mf}e^{j2\pi ft}df \quad (26)$$

In equation (26), $S(f)$ is the Fourier transform of $s(t)$. In order that the integral (26) converges, the spectrum must be a fast decreasing function. In practical applications, we can not handle either continuous functions or infinite length signals. Is it possible to compute the analytical continuation from a restricted support of the real axis ?
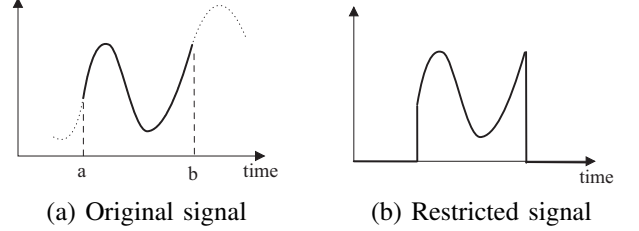

(a) Original signal   (b) Restricted signal

Fig. 1. Support restriction

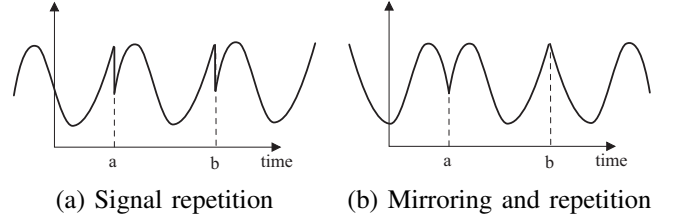(a) Signal repetition   (b) Mirroring and repetition

Fig. 2. Discontinuities

If $S(f)$ is the Fourier transform of a signal like Fig.1.b, then its spectrum will have a C/f decay. Therefore, the analytical continuation can not be computed via inverse Fourier transform. The problem is identical if the spectrum is obtained through the Discrete Fourier Transform (DFT), equation (27).

$$s(n + jm) = \sum_{k=-\frac{N}{2}+1}^{\frac{N}{2}} S(k)e^{-2\pi mk}e^{j2\pi kn} \quad (27)$$

Indeed, the spectrum is sampled involving the repetition in time of the original signal, Fig.2.a. More generally, there is a strong link between continuity of a signal and its derivatives and the decay of its Fourier transform. On the one hand, if $s \in C^p$ and if $s^{(k)} \in L^1(\mathbb{R})$ for $k \leq p$ then we have (28).

$$|S(f)| \leq \frac{\| s^{(p)} \|_1}{(2\pi|f|)^p} \quad (28)$$

On the other hand, if (28) is satisfied, then $s \in C^{p-2}$. Continuity conditions must then be ensured at the bounds of the pattern to obtain an overall continuous signal. One can easily ensure continuity of order 0, by mirroring and repeating the restricted signal. However, a necessary condition to have a fast decreasing spectrum is the continuity of all signal's derivatives. This is not guaranteed with mirroring. We can overcome this problem by applying a warping to the signal. Let's suppose we have, $s \in C^\infty[-1, 1]$ and $s(-1) \neq s(1)$. In this case, we set $a = -1$ and $b = 1$. Let's also consider a warping function defined below, (29).

$$w : t \to t_w = sin(\frac{\pi}{2}t) \quad (29)$$

4

The new defined function $\widetilde{s}(t) = s(w(t))$ is now periodical and C^∞ over the whole real axis, Fig.3. Moreover, one can expect its spectrum to be rapidly decreasing. However, proceeding this way, there is a one more little step to map the Complex Plane (CP) on which we want the signal's values and the warped complex plane. To compute $s(t + jm)$, one must compute $\widetilde{s}(\widetilde{t} + j\widetilde{m})$, which is $\widetilde{s}(\frac{2}{\pi}asin(t + jm))$, from the spectrum of $\widetilde{s}$. The correspondence between the plane is illustrated on Fig.4.

(a) Warped signal   (b) $\widetilde{s}(t)$ for $t \in \mathbb{R}$
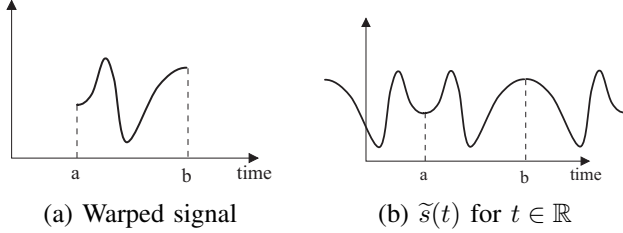
Fig. 3.   Continuous extension

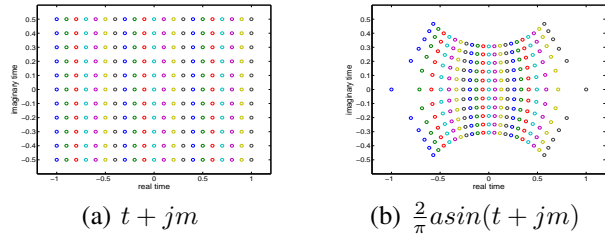(a) $t + jm$ (b) $\frac{2}{\pi}asin(t + jm)$

Fig. 4.   Complex time planes correspondance

As a result of using the Fourier transform for analytical continuation calculation, we try to have the support of the Fourier transform as compact and small as possible. The ideal case for calculation would be a Dirac in the Fourier domain. We do this for another important reason which is the presence of noise. For complex time values, the spectrum is multiplied with a very fast increasing exponential, equation (27). Reducing the spectrum support also reduces the range of this exponential and the amplification of the noise. Noise sensibility problem is described in section IV-B

Thus, in order to have a better implementation, one can try to optimize the analytical continuation calculation depending on the kind of distribution to implement. One solution based on the S-method is given in [7]. Using simple time-frequency representations as starting point for calculation is a good deal, because on the short term, the signal is usually simpler in its Fourier domain.

Example with $\widetilde{GCM_4^2}$

By using the moment (19), a distribution concentrated along instantaneous frequency rate will be obtained. To compute it, one can try to obtain $s(t + jm)$ over the needed complex plane points. Another solution is described below. One can first compute half part of the moment, (30). This part is a function of real variables and has special properties.

$$M(t, \tau) = s(t + \sqrt{\frac{\tau}{2}})s(t - \sqrt{\frac{\tau}{2}}) \qquad (30)$$

Indeed, this part of the moment also provides a distribution more or less concentrated along half the frequency rate (as much as Wigner-Ville distribution is concentrated along instantaneous frequency). This means that for a given time instant t, $\mathfrak{F}_\tau(M(t, \tau))$ is more compact than the Fourier transform of $s(t)$. Thus, it is numerically easier to compute $M(t, -\tau)$ than $s(t + j\tau)$. The computation of $M(t, -\tau)$ is still an analytical continuation calculation since we do not know $M(t, \tau)$ for negative values of τ. We can conclude that it is better to compute $\widetilde{GCM_4^2}$ by using equation (31). The computation of (30) can be done using simple interpolation algorithms like splines interpolation or even the Fourier method we used at the beginning of this section for example.

$$\widetilde{GCM_4^2}[s](t, \tau) = M(t, \tau)M(t, -\tau)^* \qquad (31)$$

This way, there is only one, instead of four, analytical continuation to compute. It should be possible to find the same kind of optimizations for the other distributions.
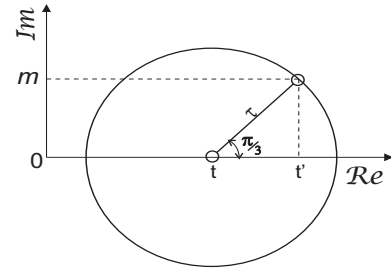

Fig. 5.   Complex time plane

One must keep in mind that the terms in equation (27) can be very large and cause numerical problems. The figure 5 depicts an example in the complex plane with one of the sixth order unity roots, when we want to compute $s(t' + jm) = s(t + \omega_{6,1}\tau)$. Without interferences, the use of large τ values should improve the accuracy of the resulting representation. However, we also go farther in the complex plane as m is increasing with τ. The maximum value of m is limited in practice, mainly by noise but also by the sampling frequency.

Instead of the DFT method, it would also be possible to directly compute an approximation of the series (13) using a polynomial modeling. However approximation of harmonic functions with polynomials requires a high modeling order. Those polynomials would not be easy to handle numerically. However, one may try to use multiprecision algorithm to tackle this problem.

B. Analytical continuation limiting factors

In presence of noise, the computation of the analytical continuation can not be done as in (27). The noise will be highly amplified for high frequencies. Thus a slight noise in the high frequency parts of the spectrum will have more effect than the powerful signal in the lowest frequencies. An example is given on figure 6. In this case, $m = 0.12$, the exponential takes high values for negative part of the spectrum.

At the beginning of the negative frequency part, the signal is correctly multiplied with the exponential. Then, as the signal has a fast decreasing spectrum, the multiplied spectrum tends toward zero. However, we observe a divergence at the end of the spectrum, which is due to the presence of noise. In this particular case, it would be easy to separate both parts of the spectrum, but when noise level is higher, it is not so obvious. An efficient filtering becomes absolutely necessary. For some cases, applying a fast decreasing windows on the spectrum could be possible but it is very tricky, mainly for two reasons. The first one is that modifying the spectrum of the signal will result in instantaneous phase modifications. The second one is that the characteristics of the window have to be adapted to the signal and to the value of m.
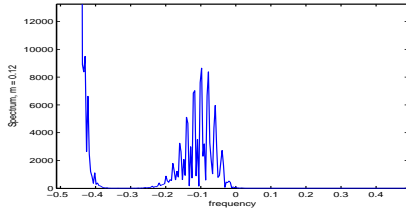

Fig. 6.   Spectrum divergence due to noise

The sampling frequency also has an influence on the calculation. Indeed, when the spectrum is multiplied with $e^{-2\pi mk}$, some parts of the spectrum are revealed depending on the value of m. This effect is shown on figure 7. The top figure shows the multiplied spectrum for $m = 0$ which is the original spectrum. As m is increasing, the maximum is shifting towards the left of the frequency axis. As long as the multiplied spectrum vanishes before the end of the frequency axis, it is not a problem. However, one can see on the bottom figure, for $m = 3$, that one part of the multiplied spectrum is missing. In this case, the analytical continuation will be miscalculated. Once again, this phenomenon is not easy to predict as it depends both on the signal and the value of m.
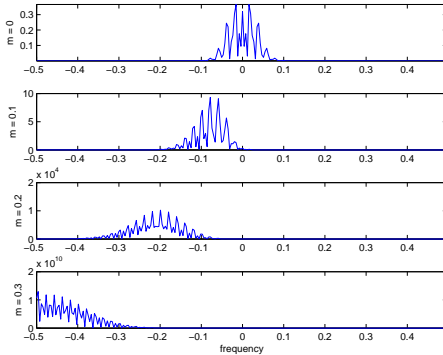

Fig. 7.   Multiplied spectra : $S(k)e^{-2\pi mk}$

As a consequence, the maximum value of m is mainly limited by the noise level but also by the sampling frequency. The method proposed in [7] for implementation is efficient to

tackle the noise problem and to deal with some multicomponent cases when the components do not cross each other. An interesting approach for implementation of the complex time distribution (CTD) is given in [8].

V. TESTS AND ILLUSTRATIONS

In this section we test the complex-time distribution by using sixth roots of unity, GCD_6^1. Theoretically, this distribution is more focused along instantaneous frequency and is numerically easier to compute than the CTD, i.e. $\widetilde{GCD_4^2}$. We will compare it to the CTD and to the Wigner-Ville distribution. We will also show an example of the same sixth order distribution concentrated along the second and third derivative of the phase. For the second order phase derivative, we will compare our distribution with $\widetilde{GCD_2^2}$, introduced by O'Shea, [3]. An example of instantaneous frequency rate estimation, using MUSIC algorithm, is given. A light smoothing is applied on each moment to improve slightly the readability of representations.

A. Signals

Distributions, introduced in this paper, will be tested on the three signals described below. The first one is a periodically frequency modulated signal with rather rapid frequency variations. Noise is added in the second signal. The last one is still a periodically modulated signal with more rapid frequency variations.

$$
\begin{aligned}
s_1(t) &= e^{j(6cos(\pi t)+\frac{4}{3}cos(3\pi t)+\frac{4}{3}cos(5\pi t))} \\
s_2(t) &= s_1(t) + n(t) \\
s_3(t) &= e^{j(10cos(\pi t)+\frac{2}{3}cos(3\pi t)+cos(9\pi t))}
\end{aligned}
$$

Note that, in the real case, these signals have the form of a radar signal produced by nonuniform rotation of reflecting point. The normalized distance changes caused by the nonuniform rotation is described by $d(t) = 6cos(\pi t) + \frac{4}{3}cos(3\pi t) + \frac{4}{3}cos(5\pi t)$ in the first signal $s_1(t)$.

B. Instantaneous frequency representation

The various time-frequency representations of $s_1(t)$ are depicted on figure 8. The WVD cannot follow the frequency variation of the signal since it is highly non linear. The result is better with the CTD because the interferences are highly reduced. However they are still visible on the picture. Some of the artifacts, around zero frequency, are due to miscalculation of the analytical continuation. The sixth order GCD exhibits a better signal representation. It is almost interferences-free and has no artifacts in this case.

The signal $s_2(t)$ is the noisy one, consisting of $s_1(t)$ and a white gaussian noise. The SNR is about 10dB. We present the WVD, the CTD and the sixth order GCD in figure 9. The last representation is still better since the sixth order GCD is naturally more robust to noise than the CTD. We observe a different shape for the WVD. It is a consequence of
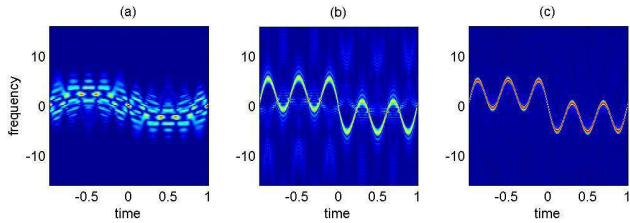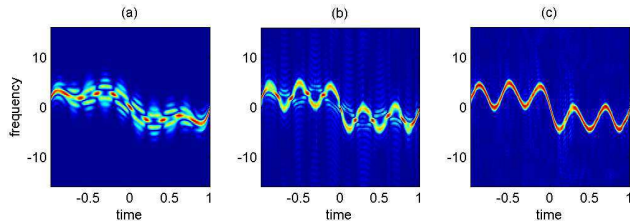
Fig. 8. (a) WVD, (b) CTD, (c) 6th GCD.

Fig. 9. SNR=10dB (a) WVD, (b) CTD, (c) 6th GCD.

a special implementation which was applied for three methods.

The last signal, $s_3(t)$, has very rapid frequency variations. It is used to show the limits of the CTD. The results are depicted in figure 10. The sixth order GCD is still well fitted to the theoretical instantaneous frequency and the interferences level is negligible compared with the WVD and the CTD.
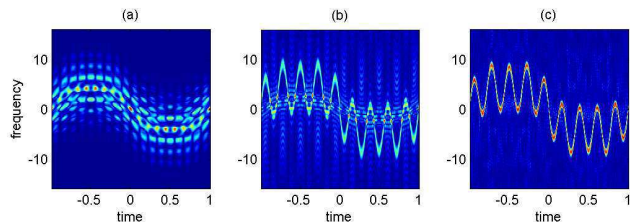

Fig. 10. (a) WVD, (b) CTD, (c) 6th GCD.

C. Second and third phase derivatives

We now tackle the problem of higher order derivatives with second and third derivatives, $K = \{2, 3\}$. With $N = 2$, it is still possible to compute instantaneous frequency rate, since we must have $K \leq N$. To illustrate the concept, we applied $\widetilde{GCM_2^2}$, $\widetilde{GCM_4^2}$ and $\widetilde{GCM_6^2}$ on $s_1(t)$. The results are depicted on figure 11. A more important smoothing is used here. On the first part of figure, (a), the representation is more spread around instantaneous frequency rate, since spreading factor Q is higher for this distribution. The second part, (b), shows some artefact on the representation due to the analytical continuation approximations. The last part, (c), represents $\widetilde{GCD_6^2}$. The accuracy is here limited by the smoothing.

Note that the third phase derivative cannot be calculated with $N = 2$. We have to use at least $N = 3$, with $\widetilde{GCM_3^3}$. We will compare it to the $\widetilde{GCM_4^3}$ and $\widetilde{GCM_6^3}$. The distributions
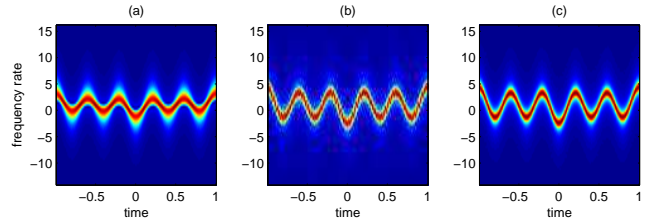

Fig. 11. $K = 2$, (a) 2nd GCD (O'shea), (b) 4th GCD, (c) 6th GCD.

are still applied on $s_1(t)$. The first shows better results than the second one, although it should theoretically be the opposite. With the smoothing, no difference can be noticed on the interferences. However, the analytical continuation of the second representation is more difficult to compute due to the fourth unity roots location, implying some artifacts on the representation. The last figure, with sixth order representation, shows better results.
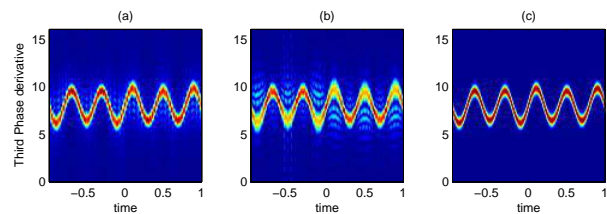

Fig. 12. $K = 3$, (a) 3rd GCD, (b) 4th GCD, (c) 6th GCD.

D. Example of instantaneous frequency rate estimation

Estimating the instantaneous frequency rate of a signal could be useful if this parameter has a physical meaning for the signal. Some methods use directly the representation to extract the parameter. With the moments introduced in this paper, we can obtain a correct concentration along the instantaneous phase derivative. In other words, for any time value, the τ variable dependent signal $\widetilde{GCM_N^K}[s](t, \tau)$ is almost monochromatic. As a consequence, it is possible to use a parametric method like MUSIC algorithm to estimate its frequency (having in mind that this frequency is related to the physical parameter we are looking for). We applied MUSIC algorithm on the three moments dedicated to frequency rate estimation. These moments were applied to $s_1(t)$. The results are depicted on figure 13. A signal without noise is used to show the accuracy of estimation for a highly non linear phase. On the picture the estimation related to sixth order moment is identical to the theoretical law. For the second order moment, results are not as good. This was expected, since on figure 11.a, the representation is not correctly focused on the frequency rate.

VI. CONCLUSION

A class of generalized complex lag distributions is proposed in this paper. These distributions are parameterized by two integers K and N. One important property is that they provide the concentration along the Kth derivative of the
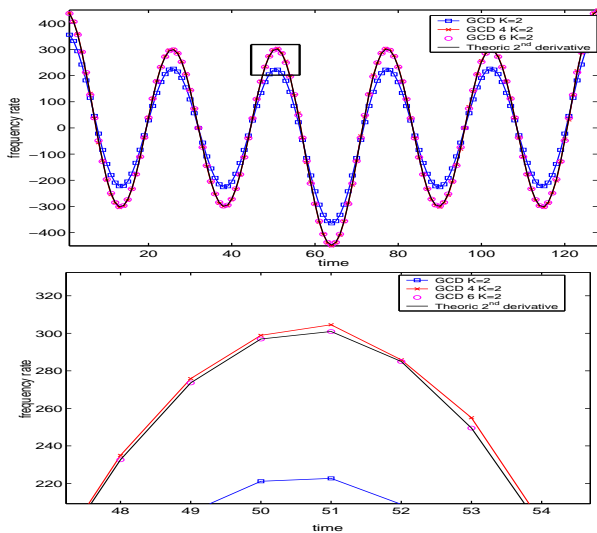
Fig. 13.   Instantaneous frequency rate estimation.

phase. In addition, it easy to generate distributions that are highly concentrated along the Kth derivative of the phase. A special case of this class of distributions, for $K = 1$, gives well known distributions for time frequency analysis. Among them, the Wigner-Ville distribution is one of the special cases. The most interesting distributions for $K = 2$ (time frequency rate analysis) and for $K = 3$ are analyzed. Theory is illustrated and justified by numerical examples.

ACKNOWLEDGMENT

REFERENCES

[1] L. Cohen, *Time-frequency analysis*.   Prentice Hall, 1995.
[2] B. Boashash, *Time-frequency signal analysis and processing*.   Elsevier, 2003.
[3] P. O'Shea, "A new technique for instantaneous frequency rate estimation," *IEEE Signal Processing Letters*, vol. 9(8), pp. 251–252, 2002.
[4] C. Cornu, S. Stankovic, C. Ioana, A. Quinquis, and L. Stankovic, "Time-frequency distributions with generalized complex lag argument," *Submitted to IEE Electronic Letters*, 2005.
[5] S. Stankovic and L. Stankovic, "Introducing time-frequency distribution with a complex-time argument," *IEE Electronic Letters*, vol. 32, no. 14, pp. 1265–1267, July 1996.
[6] W. Rudin, *Real and Complex Analysis*.   Mc Graw Hill, 1987.
[7] L. Stankovic, "Time-frequency distributions with complex argument," *IEEE Transaction on Signal Processing*, vol. 50, no. 3, pp. 475–486, March 2002.
[8] G. Viswanath and T. V. Sreenivas, "If estimation using higher order tfrs," *Signal Processing*, vol. 82, no. 2, pp. 127–132, February 2002.

8